Chemistry & Biology 13, 937–944, September 2006 ©2006 Elsevier Ltd All rights reserved DOI 10.1016/j.chembiol.2006.06.017

Alternative O-GlcNAcylation/O-Phosphorylation of Ser^{16} Induce Different Conformational Disturbances to the N Terminus of Murine Estrogen Receptor β

Yong-Xiang Chen,[1] Jin-Tang Du,[1] Lian-Xiu Zhou,[1] Xiao-Hong Liu,[1] Yu-Fen Zhao,[1] Hiroshi Nakanishi,[2] and Yan-Mei Li[1,*]

[1] Key Laboratory of Bioorganic Phosphorus Chemistry & Chemical Biology (Ministry of Education)
Department of Chemistry
Tsinghua University
Beijing 100084
China

[2] Biological Information Research Center
National Institute of Advanced Industrial Science and Technology
1-1 Higashi, Tsukuba
Ibaraki 305-8566
Japan

Summary

Serine and threonine residues in many proteins can be modified by either phosphorylation or GlcNAcylation. To investigate the mechanism of O-GlcNAc and O-phosphate's reciprocal roles in modulating the degradation and activity of murine estrogen receptor β (mER-β), the conformational changes induced by O-GlcNAcylation and O-phosphorylation of Ser^{16} in 17-mer model peptides corresponding to the N-terminal intrinsically disordered (ID) region of mER-β were studied by NMR techniques, circular dichroism (CD), and molecular dynamics simulations. Our results suggest that O-phosphorylation discourages the turn formation in the $S^{15}STG^{18}$ fragment. In contrast, O-GlcNAcylation promotes turn formation in this region. Thus, we postulate that the different changes of the local structure in the N-terminal $S^{15}STG^{18}$ fragment of mER-β caused by O-phosphate or O-GlcNAc modification might lead to the disturbances to the dynamic ensembles of the ID region of mER-β, which is related to its modulatory activity.

Introduction

Many proteins are posttranslationally modified, and the resulting modifications are often essential for the proper function of the proteins. Among the modifications, phosphorylation and 2-amino-2-deoxyglucosylation (GlcNAcylation) are unique in that they can both reversibly occur on the same Ser or Thr residues [1–4]. Therefore, it has been suggested that O-phosphorylation and O-GlcNAcylation play reciprocal roles in regulating the protein function. This reciprocal relation has been proved on several well-studied proteins, such as RNA Pol II, SV-40 large T-antigen, the c-Myc protooncogene product, and estrogen receptor β (ER-β) [1, 3, 4]. However, it is still unclear at the molecular level that how phosphorylation and GlcNAcylation can induce differences in structural and functional behavior.

*Correspondence: liym@mail.tsinghua.edu.cn

It has been shown that the O-phosphate moiety might exert both direct and indirect effects on the protein conformation leading to the changes of steric characteristic, affecting charge, and influencing the ability to form hydrogen bonds etc [5, 6]. For the O-GlcNAc modification, it was suggested that the sugar residue might transiently block phosphorylation site [3], or directly be involved in receptor binding interaction. Alternatively, it might alter the conformation of the peptide backbone [7, 8]. Wong and coworkers have concluded that O-linked GlcNAcylation serves to promote turn-like structures by studying the model peptides from the repeating C-terminal domain of RNA polymerase II [8] and mucosal addressin cell adhesion molecule-1 (MadCAM-1) [7]. In addition, recently Liang and coworkers have used a de novo designed α-helical hairpin model peptide to address the different effects of GlcNAcylation and phosphorylation on its conformational properties [9]. Here, we have explored the molecular mechanism of phosphorylation and GlcNAcylation's reciprocal roles in the regulation of protein function with peptides derived from the proteins alternatively modified with O-phosphate or O-GlcNAc moiety.

ER-β, homologous to estrogen receptor α, was discovered as a new member of the steroid hormone receptor family in 1996 [10, 11]. The estrogen receptors are the central components of the estrogen regulation and belong to the nuclear receptor (NR) gene family of transcription factors. Abnormalities in ER structure itself or ER signal transduction pathways contribute to ER-related genetic disorders such as osteoporosis, cardiovascular disease, diabetes, and cancer [11]. ER-β has a high homology to ER-α in the DNA and ligand binding domains but encodes a distinct N-terminal modulatory domain containing activation function 1 region (AF1) [12, 13]. Moreover, it was reported that the N-terminal region of ER-β possesses the same intrinsically unstructured characteristics in solution as the N-terminal transactivity region of many other NRs [12]. Since it carries out important biological functions and structural plasticity, the N-terminal region of ER-β can be postulated as an intrinsically disordered (ID) region, which lacks rigid 3D structure, existing instead as the dynamic ensembles of interconverting structures. ID proteins represent a distinct protein tribe, with disorder being an important structural element that exists at various levels, i.e., with various equilibrium constants for the order-to-disorder transition of the various ID proteins and regions [14]. Because of their structural characteristics, the widespread ID proteins are commonly involved in recognition, regulation, and cell-signaling functions [14, 15].

Hart and coworkers mapped the major O-GlcNAc site on Ser^{16} near the N terminus of murine ER-β (mER-β), which alternatively can be modified by O-phosphorylation [10, 16]. Furthermore, pulse-chase studies and luciferase reporter assays showed that the reciprocal occupancy of Ser^{16} by either an O-phosphate group or O-GlcNAc moiety modulates the degradation and activity of mER-β. It was suggested that O-phosphorylation

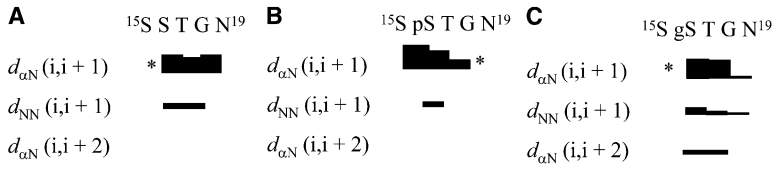

Figure 1. Summary of Important NOE Connectivities with Their Magnitudes

(A–C) OH-peptide **1** (A), OP-peptide **2** (B), and OG-peptide **3** (C). The measures were performed in aqueous solution at pH 3.5 and 278 K. Asterisks denote NOE connectivities of which the magnitudes could not be determined due to resonance overlap.

of Ser[16] accelerates degradation of mER-β, whereas O-GlcNAcylation was predicted to result in stabilization [10]. In order to explore how phosphorylation and GlcNacylation can cause different effects on mER-β, we have prepared three peptide derivatives based on the N-terminal Ala[7]-Gly[23] sequence of mER-β: the parent peptide *Ac-A[7]VMNYSVPSSTGNLEGG[23]-NH$_2$* (OH-peptide **1**), the phosphopeptide *Ac-A[7]VMNYSVPSpSTGNLEGG[23]-NH$_2$* (OP-peptide **2**), and the GlcNAcylated peptide *Ac-A[7]VMNYSVPSgSTGNLEGG[23]-NH$_2$* (OG-peptide **3**). The structures of the three peptides were studied in detail by NMR, circular dichroism (CD), and molecular dynamics simulations (MD). These studies show that the S[15]STG[18] fragment of the OH-peptide **1** containing the unmodified Ser[16] residue adopts a type II β-turn-like structure in equilibrium with random conformers. In contrast, the OP-peptide **2** adopts a more extended structure in the same region. The OG-peptide **3** adopts a type II β-turn-like conformation, and the degree of turn formation for this peptide is higher than that for the other two peptides. In addition, detailed NOE data, chemical shift perturbation data, and molecular dynamics simulation studies reveal the subtle differences in the turn structures of the three peptides. These results offer a plausible explanation of the different effects of O-phosphorylation and O-GlcNAcylation on mER-β.

Results and Discussion

NMR Resonance Assignments

Resonance assignments for the three peptides were performed with TOCSY and NOESY data by using the sequential assignment strategy, in which NMR resonances were first classified according to their amino acid spin systems in the TOCSY spectra and then unambiguously identified from sequential connectivities in the NOESY spectra [28]. The sequential assignments and chemical shifts of these three peptides are shown in the Supplemental Data (available with this article online).

The resonances of the sugar residue in OG-peptide **3** were assigned primarily based on TOCSY spectra. The amide proton of GlcNAc yielded strong TOCSY crosspeaks to two signals at 3.72 and 3.53 ppm, which were assigned to H2 and H3. Their shifts are close to the literature values for the model oligosaccharides (mean values 3.56 and 3.40 ppm) [8], and the TOCSY intensities are consistent with the expected large couplings of NH to H2 and H2 to H3. The anomeric proton of GlcNAc was well resolved at 4.59 ppm and exhibited crosspeaks to the tentatively assigned H2 and H3 resonances in the high-field quadrant of the TOCSY spectrum. The remaining GlcNAc protons were assigned by analogy with model compounds [8].

Phosphorylation and GlcNAcylation of Ser[16] Do Not Change the *cis*/*trans* Equilibria of the Prolyl Peptide Bonds in the Model Peptides

All of these three peptides have the potential to exist as two separate conformers due to the *cis*/*trans* isomerization around their Val[13]-Pro[14] prolyl peptide bonds. Prolyl *cis*/*trans* isomerization is a slow process with relaxation times of the order of ten seconds in unstructured peptides. Thus, isomerization is the rate-limiting step in many biological processes, such as protein folding and isomerspecific binding [29]. It has been reported that phosphorylation resulted in minor increases or decreases in the amount of *cis* population [30]. Wong's group has founded that the O-GlcNAc moiety did not affect the *cis*-*trans*-proline equilibrium, while the O-SLe^x group was able to shift the equilibrium [7]. For the model peptides from N-terminal of mER-β, the observation of only one clear set of resonances in the NMR spectra for each peptide and the strong $d_{\alpha\delta}$(Val[13], Pro[14]) NOEs (Supplemental Data) suggest that the prolyl peptide bond for each peptide is predominantly in the *trans* conformation. It could also be concluded that phosphorylation and GlcNAcylation of Ser[16] do not change the *cis*/*trans* equilibria of the prolyl peptide bonds in the model peptides.

NOE Data Suggest that Phosphorylation and GlcNAcylation Induce Different Structural Changes to the mER-β N-Terminal Peptide

Short- and medium-range inter- and intraresidues NOEs (Supplemental Data) between NH and αH ($d_{\alpha N}$) and between NH and NH (d_{NN}) protons define the second structure adopted by the peptides in aqueous solution. The magnitudes of the important NOE connectivities observed in these spectra are shown schematically in Figure 1.

Strong $d_{\alpha N}$(i,i+1) NOEs, which were generally observed in extended structures [31, 32], occur along most of the sequences of the three peptides. However, d_{NN}(i,i+1) or $d_{\alpha N}$(i,i+2) NOE connectivities, which are indications of helical or turn elements of structure, were only observed in the region of S[15]STG[18] containing the phosphorylation/GlcNAcylation site of Ser[16].

Two consecutive NH-NH NOEs were detected for Ser[16]-Thr[17] and Thr[17]-Gly[18] in OH-peptide **1**, while all other sequential NH-NH NOEs were too weak to be observed. In addition, significant crosspeaks at $d_{\alpha N}$(Ser[16],Thr[17]) and $d_{\alpha N}$(Thr[17],Gly[18]) were detected. Therefore, according to the NOEs description of turn structures, we propose that the fragment S[15]STG[18] adopts a turn-like structure [28, 33]. The most commonly observed reverse turns in peptide and protein structure are the four-residue β-turns. The NOEs diagnostic of β-turns include $d_{\alpha N}$(2,3), $d_{\alpha N}$(3,4), $d_{\alpha N}$(2,4), d_{NN}(2,3),

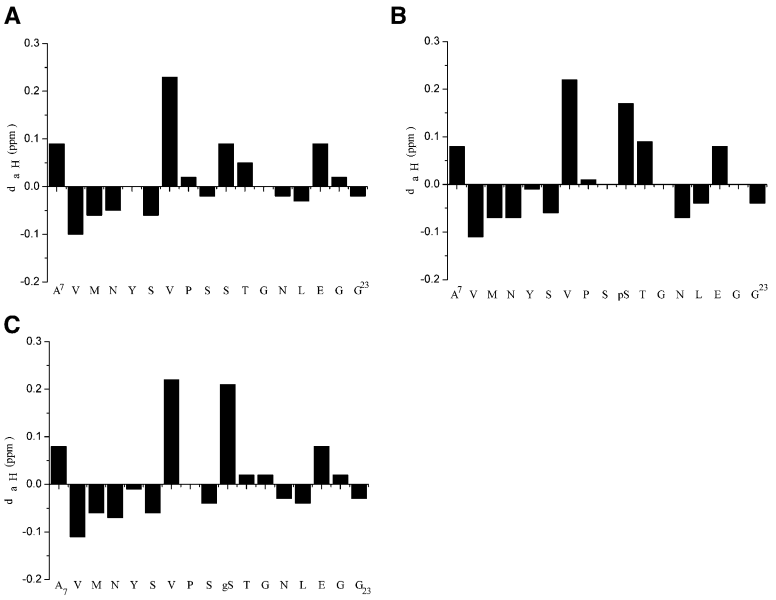

Figure 2. αH Chemical Shifts Deviations from Random Coil for OH-Peptide **1**, OP-Peptide **2**, and OG-Peptide **3**

Data were recorded at pH 3.5 and 278 K.

and d_{NN}(3,4) crosspeaks in which the numbering indicates the position in the turn [28]. Since the crosspeak at $d_{\alpha N}$(Ser^{16},Gly^{18}) is absent (Figure 1), we attribute the turn structure in S^{15}STG^{18} to a β-turn-like conformer in equilibrium with random conformers. This conclusion is also consistent with the studies [12] that the N terminus of mER-β is an intrinsically disordered (ID) region, which lacks rigid 3D structure and exists instead as dynamic ensembles of interconverting structures. It was reported that type I and type II β-turns might be distinguished by the relative strengths of the $d_{\alpha N}$(2,3) and d_{NN}(2,3) crosspeaks. Type I β-turn displays a medium $d_{\alpha N}$(2,3) crosspeak and a strong d_{NN}(2,3) crosspeak, whereas type II β-turn displays the opposite trend with a strong $d_{\alpha N}$(2,3) crosspeak and a weak d_{NN}(2,3) crosspeak [28]. However, since the coexistence of turn structure with random conformers which present strong $d_{\alpha N}$(i,i+1) NOEs, we can not attribute the β-turn in OH-peptide **1** to one specific subtype according to the relative strengths of the $d_{\alpha N}$(2,3) and d_{NN}(2,3) crosspeaks.

OP-peptide **2** and OG-peptide **3** gave different NOE signals compared with OH-peptide **1**, indicating that the local conformation in S^{15}STG^{18} region is changed upon O-phosphorylation or O-GlcNAcylation of Ser^{16}. For OP-peptide **2**, the cross peak at d_{NN}(Thr^{17},Gly^{18}) disappears (Figure 1), while crosspeaks at d_{NN}(pSer^{16},Thr^{17}), $d_{\alpha N}$(pSer^{16},Thr^{17}), and $d_{\alpha N}$(Thr^{17},Gly^{18}) are still clear in the NOE spectrum. The existence of d_{NN}(Thr^{17},Gly^{18}) could indicate that there still exist a certain amount of turn-like conformers in S^{15}STG^{18} region after the phosphorylation of Ser^{16}. However, the structure might have been changed away from a β-turn, and the degree of this turn structure might also have been changed. Thus, we propose that the O-phosphate moiety causes the local conformation near the Ser^{16} residue in mER-β to be more extended.

Analysis of the NOE spectrum of OG-peptide **3** reveals that upon O-GlcNAcylation of Ser^{16}, a new crosspeak at $d_{\alpha N}$(gSer^{16},Gly^{18}) was observed in addition to crosspeaks at $d_{\alpha N}$(gSer^{16},Thr^{17}), d_{NN}(gSer^{16}, Thr^{17}), $d_{\alpha N}$(Thr^{17},Gly^{18}), and d_{NN}(Thr^{17},Gly^{18}), indicating a more organized turn structure in the S^{15}gSTG^{18} fragment. Considering cross peaks at $d_{\alpha N}$(gSer^{16},Thr^{17}), $d_{\alpha N}$(Thr^{17},Gly^{18}), $d_{\alpha N}$(gSer^{16},Gly^{18}), d_{NN}(gSer^{16}, Thr^{17}), and d_{NN}(Thr^{17},Gly^{18}), we propose the presence of β-turn-like conformers adopted by S^{15}gSTG^{18} of OG-peptide **3** according to the NOEs diagnostic criteria of β-turns [28]. Although O-GlcNAcylation of Ser^{16} do not clearly change the structure away from the β-turn, the presence of a cross peak at $d_{\alpha N}$(gSer^{16},Gly^{18}) strongly suggests that O-GlcNAc induces the changes of local structure in the peptide backbone and apparently stabilizes the turn structure in S^{15}gSTG^{18} region. In addition, the crosspeak at $d_{\beta 1}$(gSer^{16},GlcNAc) was observed in the NOE spectrum of OG-peptide **3**, indicating that the H1 of the GlcNAc residue maintains a weak interaction with the βH of gSer^{16}. Other researchers have founded that the 2-*N*-acetamido group in GlcNAc exerted effects on the glycopeptide's conformation [34]. However, no NOESY crosspeaks between 2-amide proton in GlcNAc and protons of backbone were observed in OG-peptide **3**.

Chemical Shift Perturbations Corroborate the Changes of the Local Structure Caused by Phosphorylation and GlcNAcylation of Ser^{16}

It is established that differences in αH chemical shifts from random coil values provide an indication of the presence of a secondary structure [35, 36]. The αH chemical shifts of OH-peptide **1** and its phosphorylated/glycosylated derivatives OP-peptide **2** and OG-peptide **3** were compared to each other as well as to random coil αH chemical shifts (Figure 2). While there are small deviations (<0.1 ppm) from random coil αH chemical shifts for most residues in each peptide, the αH chemical shift for Ser^{16} in OP-peptide **2** or OG-peptide **3** is markedly different from that of Ser^{16} in OH-peptide **1**. It is likely that there still exist populations of extended conformers for all of these peptides, but local structures are changed due to phosphorylation and GlcNAcylation.

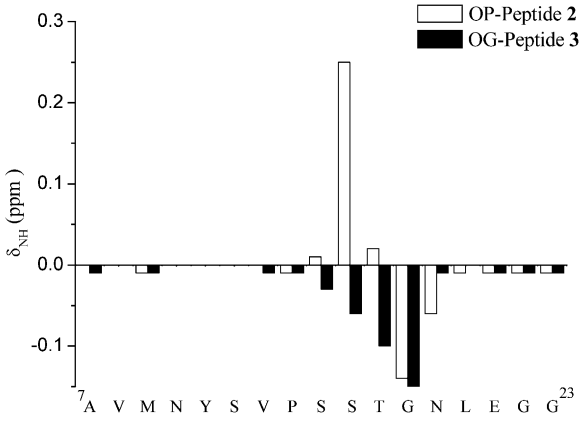

Figure 3. NH Chemical Shifts Differences from Those of OH-Peptide **1** for OP-Peptide **2** and OG-Peptide **3**

Data were recorded at pH 3.5 and 278 K. Positive values are downfield shifts, and negative values are upfield shifts.

To further investigate the subtle difference between the effects of the O-phosphate and O-GlcNAc moieties on the secondary structure of our target peptide derived from mER-β, changes of the backbone NH chemical shifts upon phosphorylation ($\delta_{\text{OP-peptide 2}}$-$\delta_{\text{OH-peptide 1}}$) and GlcNAcylation ($\delta_{\text{OG-peptide 3}}$-$\delta_{\text{OH-peptide 1}}$) were calculated for each residue (summarized in Figure 3). The NH chemical shifts can provide insights into substitution effects and are particularly sensitive to hydrogen-bonding interactions [37]. Perturbations to NH chemical shifts are indicators of secondary structure formation and can provide a method of estimating the population of folded structures [35, 36]. Therefore, differences of NH chemical shifts between OP-peptide **2** and OH-peptide **1** and between OG-peptide **3** and OH-peptide **1** are expected to reflect perturbations due to the secondary structure formation. The NH of $pSer^{16}$ in OP-peptide **2** undergoes a significant downfield shift, while there is a small upfield shift for the corresponding $gSer^{16}$ in OG-peptide **3**. As was mentioned above [29], this significant downfield shift may reflect both intrinsic effects and the formation of a hydrogen bond between the amide proton of $pSer^{16}$ and phosphate group of $pSer^{16}$. The hydrogen bond between the phosphate and amide group in a phosphopeptide has been proposed as a low-barrier hydrogen bond by Du et al. from our group and is suggested to play a role in the control of enzyme activities [38]. The upfield shift of $gSer^{16}$ NH in OG-peptide **3** may be explained by the anisotropic effect of the carbonyl group of Ser^{15}, which is forced into close proximity in the folded turn conformation [39]. Moreover, the amide protons of Thr^{17} and Gly^{18} in OG-peptide **3** shift significantly to upfield, too. It was reported that the magnitude of the NH chemical shift deviations of the corresponding residues can provide a good estimate for the degree of turn formation [40]. Thus, we propose that GlcNAcylation induces a more organized turn structure in the region of $S^{15}gSTG^{18}$.

Coupling Constants Are Likely the Ensemble Average of Turn Structures with Other Extended Conformers

Assuming a β-turn that is stably folded (100% populated) in solution, the local conformation is consistent with a coupling constant of 4 Hz $\leq {}^3J_{N\alpha} \leq$ 5 Hz. Inverse γ-turn structures are consistent with a coupling constant of 6 Hz $\leq {}^3J_{N\alpha} \leq$ 8 Hz [41]. As unstructured regions of polypeptides also display ${}^3J_{N\alpha}$ values within this range, inverse γ-turn conformations cannot be distinguished from "random coil" on the basis of coupling constants alone. ${}^3J_{N\alpha}$ coupling constants were measured through 1D ^1H NMR and DQF-COSY spectrum for all residues except Pro^{14} in the three model peptides (Supplemental Data). All the ${}^3J_{N\alpha}$ coupling constants fall into 6.0–8.0 Hz range where structural predictions are difficult to make. The coupling constants for residues near the Ser^{16} residue in each peptide are likely the ensemble average of turn structures with other extended conformers. This inference is consistent with the NOE data, which also suggests that there exist turn conformers in the $S^{15}STG^{18}$ region of each peptide in equilibrium with random conformers of different degree.

VT Coefficient Studies Confirm the Existence of Organized Structures around the Ser^{16} Residue for Each Model Peptide

Variable temperature (*VT*) coefficient is a measure of changes in the conformational equilibrium of partially folded peptides as the system is heated and the peptide goes from the folded to the random coil state [42]. Amide proton *VT* coefficient can provide information on whether an exchangeable proton is protected from solvent exchange due to hydrogen bond [43]. The *VT* studies (Table 1) indicate that the *VT* coefficients of Thr^{17} and Gly^{18} in each peptide are lower than those recorded for most other amide protons. Based on "solvent shielding" theory, these lower *VTs* are consistent with the existence of a local organized structure near the Ser^{16} residue in each peptide as an increase in folded structure would be expected to lead to an increase in the protection of the backbone NH protons from solvent exchange. Based on "equilibrium between states" [42], the lower *VTs* are consistent with shifts in the conformational equilibrium of the underlying peptide backbone. However, the small difference in *VT* coefficients (<1.0 ppb/K) for the residues around Ser^{16} in OH-peptide **1**, OP-peptide **2**, and OG-peptide **3** cannot distinguish the subtle changes in the local structures due to phosphorylation and GlcNAcylation. In addition, we found that the amide proton *VT* coefficient of Ser^{12} in each

Table 1. *VT* Coefficients of Amide Protons in OH-Peptide **1**, OP-Peptide **2**, and OG-Peptide **3**

VT	A^7	V	M	N	Y	S	V	P	S	S	T	G	N	L	E	G	G^{23}
1	6.7	8.2	7.8	6.8	8.0	4.1	7.5		8.2	7.8	5.4	4.9	5.0	6.8	5.1	5.7	5.4
2	6.2	8.2	7.8	6.8	8.0	4.1	7.5		7.9	7.2	5.2	3.9	4.7	6.8	6.1	6.3	4.6
3	6.9	8.5	7.7	7.2	8.4	4.5	7.7		8.9	6.9	4.9	5.1	5.1	7.1	6.5	6.8	5.5

VT coefficients were measured between 278 and 298 K (−Δppb/ΔK).

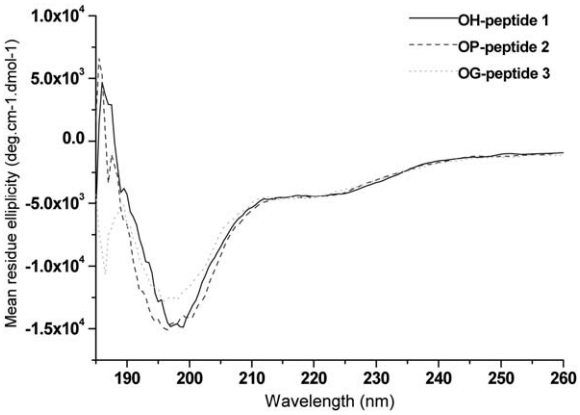

Figure 4. CD Spectra of the Three Model Peptides
The CD spectra were recorded at pH 3.5 and 298 K.

peptide is small. But based on these data, it cannot be concluded whether the amide proton of Ser^{12} in each peptide is involved in hydrogen bond or defined structure formation.

CD Studies Corroborate the Existence of Some Ordered Structures for Each Model Peptide and the Different Perturbations to the Peptide Backbone Caused by Phosphorylation and GlcNAcylation

To further study the conformation of the three model peptides, CD spectra were obtained in the region of 186–260 nm in aqueous solution (Figure 4). The spectrum for each peptide is characterized by a negative band around 198 nm attributed to disordered conformation and a negative shoulder around 220 nm indicative of the existence of some folded conformations [8, 44]. Thus, it is suggested that OH-peptide **1**, OP-peptide **2**, and OG-peptide **3** adopt defined conformers in equilibrium with random conformers. There are only small differences around 220 nm for the three peptides. However, phosphorylation of Ser^{16} shifts its negative minimum around 198 nm to slightly lower wavelength, which might be caused by the structure perturbation, while GlcNAcylation decreases the intensities of negative band at 195–200 nm considerably, indicating the decrease of the disordered structures [44].

Molecular Dynamics Simulations Reflect the Different Local Structures in the $S^{15}STG^{18}$ Region of Each Peptide

We have observed by NMR and CD that both phosphate and GlcNAc groups could influence the conformation and dynamics of the underlying peptide backbone. Molecular dynamic simulations can provide a complement method to experimental techniques used for probing the conformational space populated by OH-peptide **1**, OP-peptide **2**, and OG-peptide **3**. Moreover, they may offer insight into the subtle differences of the turn-like structures separately adopted by these three peptides, within the limits of the used force-field and simulation timescale, at an atomic level. Molecular dynamic simulations were performed on a SGI workstation with Macromodel v7.0 [27]. To reduce the computational time, the truncated models of the three model peptides, Ac-Ser^{15}-Ser-Thr-Gly-Asn^{19}-NH_2, Ac-Ser^{15}-Ser(-O-PO(OH)(O^-))-Thr-Gly-Asn^{19}-NH_2 (due to pH 3.5, the phosphate carries one negative charge), and Ac-Ser^{15}-Ser(-O-GlcNAc)-Thr-Gly-Asn^{19}-NH_2, were examined. The NOE distances (Supplemental Data) generated through the integration of crosspeaks from the NOESY spectra of the three truncated peptides were applied during molecular dynamics. In addition, the hydrogen bond between the amide proton of $pSer^{16}$ and phosphate group of $pSer^{16}$ was interpreted to the distance and angle constrains in molecular dynamics simulations of OP-peptide **2**. The amide bonds of peptide backbone were constrained in the *trans* orientation. Thirty lowest energy structures of the 100 final structures obtained from the restrained MD simulations of each truncated peptide were in superimposition (Supplemental Data). Representative structure of each of three truncated peptides is shown in Figure 5.

Consistent with the NMR measurements, molecular dynamics simulations reveal that all three truncated peptides exist in turn-like structures. For OH-peptide **1** and OG-peptide **3**, the estimation through NMR data that there exist β-turn-like conformers with different degree and subtle structure in the $S^{15}STG^{18}$ region has been confirmed by the computational modeling. It was reported that β-turns could be subdivided into a number of types based on the backbone angles φ and ψ of the residues in the loop [39]. Herein, the φ-angles and ψ-angles for i+1 and i+2 residues (i = Ser^{15}) in representative structures of all three truncated peptides were separately measured (summarized in Table 2). Based on the subcategorization standards of β-turn [45], truncated OH-peptide **1** was sorted into type II β-turn category, except that φ-angle for i+1 has a small deviation from the expected range. This observed non-ideal type II β-turn in truncated OH-peptide **1** could be caused by its engagement in equilibrium with random conformers.

Truncated OG-peptide **3** was also sorted into type II β-turn category, except that φ-angle for i+1 residue has also a small deviation from the expected range, too. It was reported that the attached carbohydrate could influence the conformation and dynamics of the underlying peptide backbone in two different ways: nonspecific steric effects or a specific peptide-sugar hydrogen bond [46]. In this case, nonspecific steric effects promote the O-GlcNAc group to be away from the plate of turn structure in $S^{15}STG^{18}$, resulting in a more stable type II β-turn like structure. On the other hand, although there was no clear hydrogen bond observed between the peptide and the sugar moiety, interactions between the peptide backbone and the sugar moiety were observed in the NOEs, which were converted to distance constrains and applied in molecular dynamics simulations. The structure representation of truncated OG-peptide **3** from constrained MD simulations supports the conclusion from NOEs data that O-GlcNAcylation stabilizes a β-turn structure around the site of Ser^{16}. Therefore, the O-GlcNAc group shifts the conformational equilibrium to the more stable β-turn, which is consistent with the notion that glycosylation serves to promote β-turn formation [7, 8, 47, 48].

According to the φ-angles and ψ-angles for i+1 and i+2 residues in truncated OP-peptide **2**, we are unable to

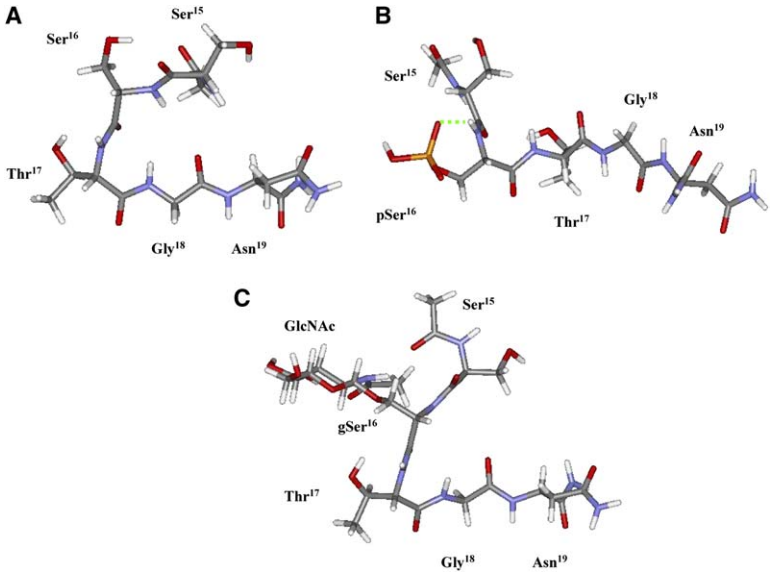

Figure 5. Representative Structures from Restrained MD Simulations of the Three Truncated Peptides

(A) Truncated OH-peptide **1**.
(B) Truncated OP-peptide **2**.
(C) Truncated OG-peptide **3**.

sort it to any subtypes of turns. However, from the simulations results, it is inferred that there exists a turn-like structure around pSer[16], although the turn is comparatively less organized than those in truncated OH-peptide **1** and OG-peptide **3**. The representative structure for OP-peptide **2** (Figure 5) shows the existence of a hydrogen bond between the amide proton of pSer[16] and the phosphate group of pSer[16] (the distance of hydrogen bond N-H---O=P is 1.99 Å, and the N-H---O angle is 138°). It is likely that this hydrogen bond affects the dihedral angles of OP-peptide **2**, which leads to a destabilization of the β-turn-like structure.

Altogether, the NMR data and the molecular dynamics simulations results suggest that the O-phosphate moiety and O-GlcNAc residue induce subtle disturbances to the local structure of the N-terminal fragment of mER-β. O-phosphorylation discourages the turn formation, and the phosphorylated peptide adopts a more extended structure. In contrast, O-GlcNAcylation promotes turn formation, and the O-GlcNAc-modified peptide adopts a more stable structure. These results are consistent with the functional observation that O-phosphorylation of mER-β promotes its degradation, while O-GlcNAcylation stabilizes the protein [10]. Perhaps O-phosphorylation causes mER-β to be more accessible to proteinases due to the lack of stable structure in the N-terminal region, while O-GlcNAcylation increases the stability of mER-β to proteolytic degradation because of secondary structure formation. Therefore, we postulate the possibility that conformational changes induced by alternative O-phosphate and O-GlcNAc modification of Ser[16] might be related to their reciprocal roles in modulating the bioactivity of mER-β.

Table 2. The φ-Angles and ψ-Angles in Representative Structures of All Three Truncated Peptides

Truncated Peptide	Φ_{i+1}	Ψ_{i+1}	Φ_{i+2}	Ψ_{i+2}
1(rep)	−148.1	121.8	60.9	14.6
2(rep)	40.1	46.5	−144.1	127.6
3(rep)	−154.0	156.7	56.6	16.8

i represents Ser[15] residue.

Significance

The reciprocal modification of Ser[16] by either O-phosphate or O-GlcNAc modulates the degradation and activity of mER-β. Here, we have explored the conformation adjusting effects of two modifications on the N-terminal intrinsically disordered (ID) region of mER-β (an activity modulatory domain) with 17-mer model peptides. The NMR, CD, and molecular dynamics simulations results show that OH-peptide 1, OP-peptide 2, and OG-peptide 3 adopt different types of turn-like structures with distinct degree in equilibrium with random conformers of the S[15]STG[18] fragments. OH-peptide 1 prefers to adopt a certain population of type II β-turn-like structure. In contrast, OP-peptide 2 adopts a more extended structure in the same region, which was hypothesized to be caused by the hydrogen bond between the amide proton of pSer[16] and the phosphate group of pSer[16]. Although the SgS[16]TG fragment of OG-peptide 3 also assumes a type II β-turn-like conformation, the O-GlcNAc group induces a change of dihedral angles around the site of Ser[16] leading to a higher degree of type II β-turn-like structure in this region. These results are consistent with the functional observations that O-phosphorylation promotes degradation of mER-β, while O-GlcNAcylation increases the stability of mER-β toward proteinases. Extrapolating these results to the full-length protein, it is likely that the changes of the local structure in the N-terminal fragment S[15]STG[18] of mER-β induced by O-phosphorylation and O-GlcNAcylation lead to the disturbance to the dynamic ensembles of the ID region of mER-β and may explain the different roles of O-phosphorylation and O-GlcNAcylation in modulating the bioactivity of mER-β. It is interesting to investigate whether similar conclusions can be drawn for other proteins that are reciprocally regulated by O-phosphorylation

and O-GlcNAcylation, such as RNA Pol II, SV-40 large T-antigen, and the c-Myc protooncogene product.

Experimental Procedures

Synthesis

The three peptides were synthesized on Rink Amide AM resin by using standard Fmoc chemistry and O-benzotriazol-N,N,N′,N′-tetramethyluronium hexafluorophosphate/1-hydroxybenzotriazol (HBTU/HOBt) coupling protocol [17]. The amino acids were commercially available except for Fmoc-Ser(Ac_3-β-O-GlcNAc)-OH, which was prepared by a literature procedure [8]. The peptides and all protecting groups except the O-acetyl groups on the N-acetyl glucosamine were cleaved from the resin with TFA containing phenol (5%), thioanisole (5%), ethanedithiol (2.5%), and water (5%) for 120 min [18]. The crude peptides were purified by reverse-phase HPLC by using an ODS-UG-5 column (Develosil) with a linear gradient of 20%–50% acetonitrile containing 0.06% trifluoroacetic acid as an ion-pairing reagent. Purified OG-peptide **3** with acetyl-protecting $GlcNAc(OAc)_3$ was deprotected by 0.1M NaOMe in methanol and finally purified by SepPak-C_{18}. The integrity of each peptide was verified by ESI-MS.

NMR Spectroscopy

Each peptide sample for NMR measurements was dissolved in H_2O/D_2O 9:1 (v/v) in 10 mM phosphate buffer. The pH value was adjusted to 3.5 by adding HCl or NaOH. Sodium 2,2-dimethyl-2-silapentonate-d_4 was used as an external standard. Standard NOESY and TOCSY experiments were collected on a Varian Inova-600 spectrometer operating at a frequency of 599.83 MHz for ^1H nucleus [19, 20]. DQF-COSY experiments were recorded to determine $^3J_{NH-\alpha H}$ coupling constants [21, 22]. Two-dimensional NMR data were transferred to an Indigo 2 (Silicon Graphics, Inc.) computer workstation and processed with the nmrPipe/nmrDraw program [23]. Usually, a sine-squared window function shifted by $\pi/4$ to $\pi/2$ was applied in both dimensions, with zero filling in f1 to 2K points. Quadrature detection in f_1 was achieved with TPPI [24]. H_2O resonance was suppressed either by presaturation of the solvent peak during the relaxation delay (and the mixing time in the NOESY spectra) or by using a pulsed-field gradient techniques with a WATERGATE sequence [25, 26]. Generally, spectra were collected with 2 K points in f_2 and 512 in f_1.

Circular Dichroism

CD spectra were recorded on a Jasco 720 spectropolarimeter from 260 to 186 nm in a 0.1 cm path length cell at room temperature. Each peptide sample was dissolved in 10 mM phosphate buffer at pH 3.5 and a concentration of about 0.2 mg/ml. Four scans were averaged. All spectra were corrected by subtracting the baseline of the solvent buffer solution recorded under the same conditions. The results were expressed as mean residue ellipticity [θ] in units of degrees $cm^2\ dmol^{-1}$.

Molecular Dynamics Simulations

Interproton distance restraints for the three peptides were generated through integration of crosspeaks from NOESY spectra acquired at 278 K. The integral volumes obtained were converted to distance restraints with the following classifications: strong (2.0 Å $\leq r_{ij} \leq$ 3.0Å), medium (2.0 Å $\leq r_{ij} \leq$ 4.0 Å), and weak (2.0 Å $\leq r_{ij} \leq$ 5.0 Å). Distance-restrained MD simulations with the GB/SA solvent and at the Amber force field were performed with Macromodel v7.0 [27] on a SGI workstation. All amide bonds were constrained in the *trans* orientation during the calculations. Energy minimization using the conjugate gradient method, to a derivative of less than 0.01 kal/Å, was performed prior to each MD calculation. This protocol consists of a total of 20 ps of molecular dynamics at 1000 K. Then, the system was cooled to 300 K over 200 ps of molecular dynamics and equilibrated for 100 ps at 300 K to generate 100 structures. Thirty lowest energy structures for each peptide were selected for further analysis. Statistical analysis, superimposition of structures, 3D graphic displays, and manipulations were achieved by using XCluster and Macromodel software.

Supplemental Data

Supplemental text, tables, and figures describing NMR and MD simulations results of OH-peptide **1**, OP-peptide **2**, and OG-peptide **3**, the synthesis rout of Fmoc-Ser-(O-β-$GlcNAc(OAc)_3COOH$), are available online at http://www.chembiol.com/cgi/content/full/13/9/937/DC1/.

Acknowledgments

This work is supported by the National Natural Science Foundation of China (No. 20472041, No. 20532020, and NSFCBIC 20320130046). We thank Prof. H. Waldman and Dr. S. Schlummer (Max-Planck-Institut für molekulare Physiologie) for help with the synthesis. We thank Dr. Y. Feng (Beijing NMR Center) for help with NMR analysis. We thank Dr. M. Sun (Tianjin Normal University) for help with Macromodel. We thank Dr. H. Lin (Cornell University) for critical reading and comments on the manuscript.

Received: April 12, 2006
Revised: June 16, 2006
Accepted: June 26, 2006
Published: September 22, 2006

References

1. Zachara, N.E., and Hart, G.W. (2002). The emerging significance of O-GlcNAc in cellular regulation. Chem. Rev. *102*, 431–438.
2. Vosseller, K., Sakabe, K., Wells, L., and Hart, G.W. (2002). Diverse regulation of protein function by O-GlcNAc: a nuclear and cytoplasmic carbohydrate post-translational modification. Curr. Opin. Chem. Bio. *6*, 851–857.
3. Wells, L., Vosseller, K., and Hart, G.W. (2001). Glycosylation of nucleocytoplasmic proteins: signal transduction and O-GlcNAc. Science *291*, 2376–2378.
4. Comer, F.I., and Hart, G.W. (2000). O-glycosylation of nuclear and cytosolic proteins. J. Biol. Chem. *275*, 29179–29182.
5. Tholey, A., Lindemann, A., Kinzel, V., and Reed, J. (1999). Direct effects of phosphorylation on the preferred backbone conformation of peptides: a nuclear magnetic resonance study. Biophys. J. *76*, 76–87.
6. Du, J.T., Li, Y.M., Ma, Q.F., Qiang, W., Zhao, Y.F., Abe, H., Kanazawa, K., Qin, X.R., Aoyagi, R., Ishizuka, Y., et al. (2005). Synthesis and conformational properties of phosphopeptides related to the human tau protein. Regul. Pept. *130*, 48–56.
7. Wu, W.G., Pasternack, L., Huang, D.H., Koeller, K.M., Lin, C.C., Seitz, O., and Wong, C.H. (1999). Structural study on O-glycopeptides: glycosylation-induced conformational changes of O-GlcNAc, O-LacNAc, O-sialyl-LacNAc, and O-sialyl-lewis-X peptides of the mucin domain of MAdCAM-1. J. Am. Chem. Soc. *121*, 2409–2417.
8. Simanek, E.E., Huang, D.H., Pasternack, L., Machajewski, T.D., Seitz, O., Millar, D.S., Dyson, H.J., and Wong, C.H. (1998). Glycosylation of threonine of the repeating unit of RNA polymerase II with beta-linked N-acetylglucosame leads to a turnlike structure. J. Am. Chem. Soc. *120*, 11567–11575.
9. Liang, F.C., Chen, R.P.Y., Lin, C.C., Huang, K.T., and Chan, S.I. (2006). Tuning the conformation properties of a peptide by glycosylation and phosphorylation. Biochem. Biophys. Res. Commun. *342*, 482–488.
10. Cheng, X.G., and Hart, G.W. (2001). Alternative O-glycosylation/O-phosphorylation of serine-16 in murine estrogen receptor beta: post-translational regulation of turnover and transactivation activity. J. Biol. Chem. *276*, 10570–10575.
11. Pettersson, K., and Gustafsson, J.A. (2001). Role of estrogen receptor beta in estrogen action. Annu. Rev. Physiol. *63*, 165–192.
12. Warnmark, A., Wikstrom, A., Wright, A.P.H., Gustafsson, J.A., and Hard, T. (2001). The N-terminal regions of estrogen receptor alpha and beta are unstructured in vitro and show different TBP binding properties. J. Biol. Chem. *276*, 45939–45944.
13. European Bioinformatics Institute (2006). IPR012239 oestrogen receptor (http://www.ebi.ac.uk/interpro/DisplayIproEntry?ac=IPR012239)

14. Uversky, V.N., Oldfield, C.J., and Dunker, A.K. (2005). Showing your ID: intrinsic disorder as an ID for recognition, regulation and cell signaling. J. Mol. Recognit. *18*, 343–384.
15. Fink, A.L. (2005). Natively unfolded proteins. Curr. Opin. Struct. Biol. *15*, 35–41.
16. Cheng, X.G., Cole, R.N., Zaia, J., and Hart, G.W. (2000). Alternative O-glycosylation/O-phosphorylation of the murine estrogen receptor beta. Biochemistry *39*, 11609–11620.
17. Fields, G.B., and Noble, R.L. (1990). Solid phase peptide synthesis utilizing 9-fluorenylmethoxycarbonyl amino acids. Int. J. Pept. Protein Res. *35*, 161–214.
18. Muhlradt, P.F., Kiess, M., Meyer, H., Sussmuth, R., and Jung, G. (1997). Isolation, structure elucidation, and synthesis of a macrophage stimulatory lipopeptide from Mycoplasma fermentans acting at picomolar concentration. J. Exp. Med. *185*, 1951–1958.
19. Bax, A.D., and Davis, D.G. (1985). Practical aspects of two-dimenisional transverse NOE spectroscopy. J. Magn. Reson. *63*, 207–213.
20. Macura, S., and Ernst, R.R. (1980). Elucidation of cross-relaxation in liquids by two-dimensional NMR spectroscopy. Mol. Phys. *41*, 95–117.
21. Redfield, A.G., and Kunz, S.D. (1975). Quadrature Fourier NMR detection—simple multiplex for dual detection and discussion. J. Magn. Reson. *19*, 250–254.
22. Rance, M., Sorensen, O.W., Bodenhausen, G., Wagner, G., Ernst, R.R., and Wuethrich, K. (1983). Improved spectral resolution in cosy 1H NMR spectra of proteins via double quantum filtering. Biochem. Biophys. Res. Commun. *117*, 479–495.
23. Delaglio, F., Grzesiek, S., Vuister, G.W., Zhu, G., Pfeifer, J., and Bax, A. (1995). Nmrpipe—a multidimensional spectral processing system based on unix pipes. J. Biomol. NMR *6*, 277–293.
24. Marion, D., and Wüthrich, K. (1983). Application of phase sensitive two-dimensional correlated spectroscopy (COSY) for measurements of 1H-1H spin-spin coupling constants in proteins. Biochem. Biophys. Res. Commun. *113*, 967–974.
25. Kay, L.E. (1995). Pulsed field gradient multi-dimensional NMR methods for the study of protein structure and dynamics in solution. Prog. Biophys. Mol. Biol. *63*, 277–299.
26. Piotto, M., Saudek, V., and Sklenar, V. (1992). Gradient-tailored excitation for single-quantum NMR spectroscopy of aqueous solutions. J. Biomol. NMR *2*, 661–665.
27. Mohamadi, F., Richards, N.G.J., Guida, W.C., Liskamp, R., Lipton, M., Caufield, C., Chang, G., Hendrickson, T., and Still, W.C. (1990). Macromodel—an integrated software system for modeling organic and bioorganic molecules using molecular mechanics. J. Comput. Chem *11*, 440–467.
28. Wuethrich, K. (1986). NMR of Protein and Nucleic Acids (New York, NY: Wiley-Interscience).
29. Ramelot, T.A., and Nicholson, L.K. (2001). Phosphorylation-induced structural changes in the amyloid precursor protein cytoplasmic tail detected by NMR. J. Mol. Biol. *307*, 871–884.
30. Schutkowski, M., Bernhardt, A., Zhou, X.Z., Shen, M., Reimer, U., Rahfeld, J.U., Lu, K.P., and Fischer, G. (1998). Role of phosphorylation in determining the backbone dynamics of the serine/threonineproline motif and Pin1 substrate recognition. Biochemistry *37*, 5566–5575.
31. Dyson, H.J., Rance, M., Houghten, R.A., Wright, P.E., and Lerner, R.A. (1988). Folding of immunogenic peptide fragments of proteins in water solution. J. Mol. Biol. *201*, 201–217.
32. Dyson, H.J., and Wright, P.E. (1991). Defining solution conformations of small linear peptides. Annu. Rev. Biophys. Chem. *20*, 519–538.
33. Dettin, M., Falcigno, L., Campanile, T., Scarinci, C., D'Auria, G., Cusin, M., Paolillo, L., and Di Bello, C. (2001). A type-II beta-turn, proline-containing, cyclic pentapeptide as a building block for the construction of models of the cleavage site of pro-oxytocin. J. Pept. Sci. *7*, 358–373.
34. Palian, M.M., Jacobsen, N.E., and Polt, R. (2001). O-linked glycopeptides retain helicity in water. J. Pept. Res. *58*, 180–189.
35. Wishart, D.S., Sykes, B.D., and Richards, F.M. (1991). Relationship between nuclear magnetic resonance chemical shift and protein secondary structure. J. Mol. Biol. *222*, 311–333.
36. Wishart, D.S., Sykes, B.D., and Richards, F.M. (1992). The chemical shift index: a fast and simple method for the assignment of protein secondary structure through NMR spectroscopy. Biochemistry *31*, 1647–1651.
37. McManus, A.M., Otvos, L., Hoffmann, R., and Craik, D.J. (1999). Conformational studies by NMR of the antimicrobial peptide, drosocin, and its non-glycosylated derivative: effects of glycosylation on solution conformation. Biochemistry *38*, 705–714.
38. Du, J.T., Li, Y.M., Wei, W., Wu, G.S., Zhao, Y.F., Kanazawa, K., Nemoto, T., and Nakanishi, H. (2005). Low-barrier hydrogen bond between phosphate and the amide group in phosphopeptide. J. Am. Chem. Soc. *127*, 16350–16351.
39. Griffiths-Jones, S.R. (2005). The role of beta-turns in beta-sheets (http://www.sanger.ac.uk/users/sgj/thesis/html/node34.html).
40. Maynard, A.J., Sharman, G.J., and Searle, M.S. (1998). Origin of beta-hairpin stability in solution: structural and thermodynamic analysis of the folding of model peptide supports hydrophobic stabilization in water. J. Am. Chem. Soc. *120*, 1996–2007.
41. Karplus, M. (1959). Contact electron-spin coupling of nuclear magnetic moments. J. Chem. Phys. *30*, 11–15.
42. Andersen, N.H., Neidigh, J.W., Harris, S.M., Lee, G.M., Liu, Z.H., and Tong, H. (1997). Extracting information from the temperature gradients of polypeptide NH chemical shifts. 1. The importance of conformational averaging. J. Am. Chem. Soc. *119*, 8547–8561.
43. Bosques, C.J., Tschampel, S.M., Woods, R.J., and Imperiali, B. (2004). Effects of glycosylation on peptide conformation: a synergistic experimental and computational study. J. Am. Chem. Soc. *126*, 8421–8425.
44. Schlosser, G., Mezo, G., Kiss, R., Vass, E., Majer, Z., Feijlbrief, M., Perczel, A., Bosze, S., Welling-Wester, S., and Hudecz, F. (2003). Synthesis, solution structure analysis and antibody binding of cyclic epitope peptides from glycoprotein D of Herpes simplex virus type I. Biophys. Chem. *106*, 155–171.
45. Wilmot, C.M., and Thornton, J.M. (1988). Analysis and prediction of the different types of beta-turn in proteins. J. Mol. Biol. *203*, 221–232.
46. Schuman, J., Campbell, A.P., Koganty, R.R., and Longenecker, B.M. (2003). Probing the conformational and dynamical effects of O-glycosylation within the immunodominant region of a MUC1 peptide tumor antigen. J. Pept. Res. *61*, 91–108.
47. Kirnarsky, L., Prakash, O., Vogen, S.M., Nomoto, M., Hollingsworth, M.A., and Shermin, S. (2000). Structural effects of O-glycosylation on a 15-residue peptide from the mucin (MUC1) core protein. Biochemistry *39*, 12076–12082.
48. Naganagowda, G.A., Gururaja, T.L., Styanarayana, J., and Levine, M.J. (1999). NMR analysis of human salivary mucin (MUC7) derived O-linked model glycopeptides: comparison of structural features and carbohydrate-peptide interactions. J. Pept. Res. *54*, 290–310.